PHYSICAL REVIEW B VOLUME 42, NUMBER 2 15 JULY 1990-I

Electronic states in *trans*-polyacetylene with bond-type impurities in the coherent-potential approximation

Kikuo Harigaya and Yasushi Wada
Department of Physics, University of Tokyo, 7-3-1 Hongo, Bunkyo-ku, Tokyo 113, Japan

Klaus Fesser
Physikalisches Institut, Universität Bayreuth, Postfach 10 12 51, D-8580 Bayreuth, Federal Republic of Germany
(Received 19 June 1989; revised manuscript received 19 March 1990)

Disorder effects on the electronic states in *trans*-polyacetylene are investigated in the case of bond-type impurities which give rise to backward scatterings of electrons. The generalized Takayama–Lin-Liu–Maki model is studied with the help of the coherent-potential approximation (CPA). The dimerization of the lattice is assumed to be uniform and is represented by an order parameter Δ. The CPA gives equations for electron Green functions. They are solved numerically, while Δ is determined as to give minimum energy. We find three solutions at low impurity concentrations, one of which is stable solution, another is metastable, while the third is unstable. In the stable solution, which survives for higher impurity concentrations, impurity bands are not formed. In the metastable solution, the conduction and valence bands intrude into the gap region, indicating the development of impurity bands. Concentration dependences of the order parameters, energy gaps, and the critical concentration for the metastable solution are derived.

I. INTRODUCTION

It has been well known that doping of *trans*-polyacetylene dramatically increases its electrical conductivity.[1] Metallic Pauli susceptibility has been observed only after the dopant concentration becomes larger than a few percent. In the lightly doped polyacetylene, the conductivity is high without the Pauli susceptibility. The conduction is performed by spinless charged carriers. It has been proposed that charged solitons are playing a role. Some mechanisms have been considered: electron hopping between charged and neutral solitons[2] and thermally excited motion of charged solitons trapped by dopants.[3] On the other hand, the mechanism without solitons might also be possible. The variable range hopping among the localized levels around dopants[4] has been suggested. It is therefore necessary to investigate the electronic structures of doped polyacetylene in order to identify the most effective mechanism of the conduction.

The effect of a single impurity has been extensively studied by Phillpot, Baeriswyl, Bishop, and Lomdahl.[5] They have investigated two types of impurities. One is the site-type impurity, for which the site energy of π electrons is locally modulated around the charged impurity. Dopant atoms would release or accept electrons to become the charged impurities whose Coulomb potentials would modulate the site energy. The other is the bond-type impurity, for which the electronic transfer integral is randomly modulated. One example of the bond impurity would be *cis* segments embedded in a *trans* chain. The other would be the change in the distance between neighboring CH units due to nonhomogeneous distributions of charged impurities. The many-impurity problem has been studied, using the generalized Takayama–Lin-Lui–Maki (TLM) model.[6] Xu and Trullinger have made use of the supersymmetry technique.[7] We have used Eilenberger equations, trying to incorporate solitons and polarons into the discussion.[8,9] A drawback of both methods has been the fact that the impurity effects are taken into account only by the Born approximation. Thus, the possiblity of studying the impurity bands, if there are any, is automatically excluded.

Terai has taken another approach, using a generalized Su-Schrieffer-Heeger (SSH) model.[10] He has solved the problem numerically, assuming a uniform order parameter, to find the reduction in the order parameter and the energy gap with increasing disorder. He has observed new electronic states in the intragap region and beyond the band edges as well.

The purpose of this paper is to investigate the electronic states of the *trans*-polyacetylene doped with the bond-type impurities, with the help of the coherent-potential approximation. This method takes into account the electron scattering by the impurities rigorously in an effective potential by the other impurities. The potential is determined self-consistently. This method was fully developed and applied for various disordered systems successfully. In particular, the structures of impurity bands are extensively explored in doped semiconductors. It is highly possible that this method is similarly effective for conducting polymers.

In this work, we make some simplifications. The lattice is assumed to be perfectly dimerized. The dimerization pattern is uniform. It is known that the doping induces solitons and polarons which disrupt this pattern.[5,11] It would not be straightforward, however, to take into account such large disruptions in the coherent-potential approximation which takes an average over the disorders. We further assume that half of the electronic states are filled. The doping usually changes the electron density. At low doping levels, it would modulate the perfect dimerization into a soliton lattice. To avoid the complexity, we suppose the doping is compensated to keep the electron number unchanged.

The magnitude of the dimerization is denoted by a parameter Δ which is determined to give stationary values of the total energy. We find three stationary values. For each value, the impurity concentration dependences of Δ, energy gap, and the total energy are calculated. The electronic density of states is estimated to find that the stable solution has no impurity band in the energy gap. The gap increases with the impurity concentration. This absence of impurity band is characteristic to the quasi-one-dimensional systems under consideration.

In Sec. II, we present the model and discuss the electronic states around the single impurity. The coherent potential approximation is reviewed in Sec. III. Numerical results are presented in Sec. IV and qualitative features of the solutions and remaining problems are discussed in Sec. V.

II. SINGLE-IMPURITY PROBLEM

In the previous papers,[8,9] we have discussed the effects of impurities in *trans*-polyacetylene, using the generalized Takayama-Lin-Liu-Maki model[6]

$$H=H_{\rm TLM}+H_{\rm imp}\ , \tag{2.1}$$

$$H_{\rm TLM}=\sum_s\int dx\,\Psi_s^\dagger(x)\left[-iv_F\sigma_3\frac{\partial}{\partial x}+\sigma_1\Delta(x)\right]\Psi_s(x)+\frac{1}{2\pi\lambda v_F}\int dx\,\Delta^2(x)\ , \tag{2.1a}$$

$$H_{\rm imp}=U\sum_i\sum_s\int dx\,\Psi_s^\dagger(x)\delta(x-x_i)\sigma_1\Psi_s(x)\ , \tag{2.1b}$$

where $\Psi_s(x)$ is a two-component field operator of electrons with spin s, σ_i are the Pauli spin matrices, $\Delta(x)$ is the order parameter, v_F is the Fermi velocity, and λ is the dimensionless electron-phonon coupling constant. The coordinate x_i is the location of the ith impurity. The impurities are distributed randomly. The strength of the short-range impurity potential is denoted by U. The impurity Hamiltonian $H_{\rm imp}$, (2.1b), modifies the electron transfer which is associated with σ_1. Therefore we name the impurities bond type; in another terminology it gives rise to backward scatterings of electrons. The electrons moving to the right are scattered to propagate to the left, and vice versa. Model (2.1) has been studied with the help of the self-consistent Born approximation. We first examine the single-impurity problem with a uniform order parameter $\Delta(x)=\Delta_0$. Introducing the Fourier transform by

$$\Psi_s(x)=\frac{1}{\sqrt{L}}\sum_k e^{ikx}\Psi_s(k)\ ,$$

where L is the system size, we define the temperature Green function in the impurity-free system by

$$G_s^{(0)}(k,\tau)=-\langle T_\tau[\Psi_s(k,\tau)\Psi_s^\dagger(k,0)]\rangle_0\ , \tag{2.2}$$

where

$$\Psi_s(k,\tau)=\exp(H_{\rm TLM}\tau)\Psi_s(k)\exp(-H_{\rm TLM}\tau)\ .$$

Its Fourier transform with respect to τ is

$$G_s^{(0)}(k,iE_n)=(iE_n-v_Fk\sigma_3-\Delta_0\sigma_1)^{-1}\ , \tag{2.3}$$

where $E_n=(2n+1)\pi T$ is the Matsubara frequency. The Green function for the system with one impurity is defined by

$$G_s(k,p,\tau)=-\langle T_\tau[\tilde{\Psi}_s(k,\tau)\tilde{\Psi}_s^\dagger(p,0)]\rangle\ , \tag{2.4}$$

where $\tilde{\Psi}_s(k,\tau)=\exp(H\tau)\Psi_s(k)\exp(-H\tau)$. Its Fourier transform satisfies the equation of motion

$$G_s^{(0)-1}(k,iE_n)G_s(k,p,iE_n)=\delta_{k,p}+\frac{U}{L}\sum_{k'}\exp[i(k'-k)x_0]\sigma_1G_s(k',p,iE_n)\ , \tag{2.5}$$

where x_0 is the coordinate of the impurity. We define a scattering t matrix $t(iE_n)$ by the relation

$$G_s(k,p,iE_n)=\delta_{k,p}G_s^{(0)}(k,iE_n)+G_s^{(0)}(k,iE_n)t(iE_n)G_s^{(0)}(p,iE_n)\ . \tag{2.6}$$

Equation (2.5) gives

$$t(iE_n)=\frac{U\sigma_1}{L}\frac{\exp[i(p-k)x_0]}{1-\frac{U}{L}\sum_{k'}G_s^{(0)}(k',iE_n)\sigma_1}\ . \tag{2.7}$$

Using (2.3), we obtain

$$\frac{1}{L}\sum_{k'}G_s^{(0)}(k',iE_n)=-\frac{iE_n+\Delta_0\sigma_1}{2v_F[\Delta_0^2-(iE_n)^2]^{1/2}}\ . \tag{2.8}$$

Substitution into (2.7) gives

$$t(\omega)=\frac{U\sigma_1}{L}\frac{2v_F(\Delta_0^2-\omega^2)^{1/2}[2v_F(\Delta_0^2-\omega^2)^{1/2}+U\Delta_0-\omega U\sigma_1]}{[2v_F(\Delta_0^2-\omega^2)^{1/2}+U\Delta_0]^2-U^2\omega^2}\exp[i(p-k)x_0]\ , \tag{2.9}$$

where iE_n is replaced by ω. Localized levels around the impurity are given by the singularities of $t(\omega)$. They are determined by

$$(\Delta_0^2-\omega^2)^{1/2}=-\frac{4v_F U\Delta_0}{4v_F^2+U^2} . \tag{2.10}$$

If $U\Delta_0$ is positive, the two sides of (2.10) have opposite signs. It does not have a real root, and there are no localized levels. When $U\Delta_0$ is negative, there are two levels at

$$\omega=\pm\Delta_0\left[\frac{4v_F^2-U^2}{4v_F^2+U^2}\right] . \tag{2.11}$$

Due to the electron-hole symmetry, the two levels are at the symmetric positions with respect to $\omega=0$.

This result is similar to that of the single impurity with backward scattering in the system of a charge-density wave.[12]

III. COHERENT-POTENTIAL APPROXIMATION

Various approximation methods have been developed to study the effects of randomly distributed impurities. For instance, Shiba proposed a method to use the t matrix (2.7) for the self-energy part in which the Green function $G_s^{(0)}$ in the denominator was replaced by a Green function which was determined self-consistently.[13] Then, the Soven-Taylor coherent-potential approximation (CPA) was widely used.[14] It reduces to Shiba's method if the impurity concentration is dilute. We briefly review the CPA, applying it to the present problem. The temperature Green function $G_s(k,p,iE_n)$ satisfies the following equation of motion:

$$(iE_n-v_Fk\sigma_3-\sigma_1\Delta)G_s(k,p,iE_n)=\delta_{k,p}+\frac{I}{N}\sum_i\sum_{k'}\exp[i(k'-k)x_i]\sigma_1 G_s(k',p,iE_n) , \tag{3.1}$$

where a uniform order parameter $\Delta(x)=\Delta$ is assumed and $L=2aN$ with $U=2aI$. The continuum system is simulated by a discrete system with N sites, $2a$ being the lattice constant where a is the spacing of the undimerized lattice of the Su-Schrieffer-Heeger (SSH) model. Equation (3.1) is the generalization of (2.5) to the system with many impurities. Defining the $G_k^{(0)-1}$, G_{kp}, and $V_{kk'}$ by

$$G_k^{(0)-1}=iE_n-v_Fk\sigma_3-\sigma_1\Delta , \tag{3.2a}$$

$$G_{kp}=G_s(k,p,iE_n) , \tag{3.2b}$$

$$V_{kk'}=\frac{I}{N}\sum_i\exp[i(k'-k)x_i]\sigma_1 , \tag{3.2c}$$

we rewrite it as

$$G_k^{(0)-1}G_{kp}=\delta_{k,p}+\sum_{k'}V_{kk'}G_{k'p} , \tag{3.3}$$

which can be written symbolically as

$$G^{(0)-1}G=1+VG . \tag{3.3a}$$

We introduce the coherent potential S through

$$(G^{(0)-1}-S)G=1+(V-S)G . \tag{3.4}$$

This coherent potential S is to be chosen so that the effective medium Green function $\overline{G}$, which is the average of G over the impurity distribution, is identical with $(G^{(0)-1}-S)^{-1}$. Then, Eq. (3.4) becomes

$$G=\overline{G}+\overline{G}T\overline{G} , \tag{3.5}$$

where the t matrix T is given by

$$T=(V-S)[1-\overline{G}(V-S)]^{-1} . \tag{3.6}$$

Since the average of G is $\overline{G}$ itself, Eq. (3.5) indicates that the average of T should vanish:

$$\overline{T}=0 . \tag{3.7}$$

In the site representation, the quantity $V_{kk'}$ is transformed to

$$V_{nm}=\frac{1}{N}\sum_{k,k'}\exp[i(kx_n-k'x_m)]V_{kk'} , \tag{3.8}$$

where $x_m=2ma$. It becomes diagonal, $V_{mn}=\delta_{mn}V_n$, and its diagonal element is given by

$$V_n=I\sigma_1\xi_n , \tag{3.9}$$

where ξ_n is a random variable defined by

$$\xi_n=\begin{cases}1 & \text{if one of } x_i\text{'s is at } 2na,\\ 0 & \text{otherwise} .\end{cases} \tag{3.10}$$

Site representations of T and S are similarly introduced by

$$T_{mn}=\frac{1}{N}\sum_{k,p}\exp[i(kx_m-px_n)]T_{kp} \tag{3.11a}$$

and

$$S_{mn}=\frac{1}{N}\sum_{k,p}\exp[i(kx_m-px_n)]S_{kp} . \tag{3.11b}$$

In the single-site CPA,[14] the coherent potential is assumed to be site diagonal as well:

$$S_{mn}=\delta_{mn}\Sigma . \tag{3.12}$$

The quantity Σ is independent of n, since S is a quantity averaged over the impurity distribution. From (3.11b) and (3.12), we find $S_{kp}=\delta_{kp}\Sigma$. This means that $\overline{G}$ is a diagonal matrix in momentum space

$$\overline{G}_{kp}=[(G^{(0)-1}-S)^{-1}]_{kp}=\delta_{kp}(G_k^{(0)-1}-\Sigma)^{-1} . \tag{3.13}$$

The denominator of (3.6) is expanded in the site representation to give

$$T_{mn}=\delta_{mn}(V_m-\Sigma)+(V_m-\Sigma)\overline{G}_{mn}(V_n-\Sigma)+\sum_{l}(V_m-\Sigma)\overline{G}_{ml}(V_l-\Sigma)\overline{G}_{ln}(V_n-\Sigma)+\cdots\;, \tag{3.14}$$

where

$$\overline{G}_{mn}=\frac{1}{N}\sum_{k}\exp[ik(x_m-x_n)]\overline{G}_{kk}\;.$$

In the single site approximation, we retain only the terms which correspond to multiple scatterings from the same site without recourse to other sites. Off-diagonal elements of T_{mn} are neglected, while the diagonal elements are given by

$$T_{mn}=\delta_{mn}t_n\;, \tag{3.15}$$

where

$$t_n=(V_n-\Sigma)[1-\overline{g}(V_n-\Sigma)]^{-1}\;. \tag{3.16}$$

Here, $\overline{g}$ is site diagonal and defined by

$$\overline{g}=\overline{G}_{nn}=\frac{1}{N}\sum_{k}\overline{G}_{kk}\;. \tag{3.17}$$

Equation (3.7) is now rewritten, with the help of (3.9), (3.15), and (3.16):

$$\begin{aligned}\overline{T}_{nn}&=\frac{1}{N}\sum_{n}t_n\\&=c(I\sigma_1-\Sigma)[1-\overline{g}(I\sigma_1-\Sigma)]^{-1}\\&\quad-(1-c)\Sigma[1+\overline{g}\Sigma]^{-1}\\&=0\;,\end{aligned} \tag{3.18}$$

where c is the concentration of impurities. The average of t_n over the impurity distribution is replaced by the average over the sites in the effective medium.

Because of the symmetry between electrons moving in positive and negative directions, the diagonal elements in Σ should be the same. Moreover, we can show that Eq. (3.18) has a solution of the form

$$\Sigma(iE_n)=\Sigma_1(iE_n)1+\Sigma_2(iE_n)\sigma_1\;. \tag{3.19}$$

After analytic continuation to the real axis $\Sigma(iE_n)\rightarrow\Sigma(\omega+i\delta), \overline{g}(iE_n)\rightarrow\overline{g}(\omega+i\delta)$, we perform the k integral in (3.17) to get

$$\overline{g}(\omega+i\delta)=g_1(\omega)1+g_2(\omega)\sigma_1\;, \tag{3.20}$$

where

$$\frac{g_1(\omega)}{\omega-\Sigma_1(\omega)}=\frac{g_2(\omega)}{\Delta+\Sigma_2(\omega)}=-\frac{1}{4\pi t_0 r(\omega)}\left[\mathrm{Ln}\left[\frac{v_F\Lambda-r(\omega)}{-v_F\Lambda-r(\omega)}\right]-\mathrm{Ln}\left[\frac{v_F\Lambda+r(\omega)}{-v_F\Lambda+r(\omega)}\right]\right]\;, \tag{3.21a}$$

and

$$r(\omega)=[(\omega-\Sigma_1)^2-(\Delta+\Sigma_2)^2]^{1/2}\;. \tag{3.21b}$$

Here, $v_F=2at_0$ as in the SSH model, the quantity $\Lambda=a^{-1}$ is the cutoff for the k integral, and the notation Ln means the principal value. The square root is defined such that $\mathrm{Im}r(\omega)>0$ at the real axis. The condition for the coherent potential, (3.18), is now written

$$\Sigma=(cI\sigma_1-\Sigma\overline{g}\Sigma)(1-\overline{g}I\sigma_1)^{-1}\;. \tag{3.22}$$

It gives two equations which determine $\Sigma_1(\omega)$ and $\Sigma_2(\omega)$ in terms of $g_i(\omega)$'s. They are to be solved in accordance with the analyticity conditions discussed in Appendix A. Equations (3.21a) and (3.22) have to be investigated numerically, together with the self-consistency equation

$$\sum_{s}\int dx\langle\Psi_s^{\dagger}(x)\sigma_1\Psi_s(x)\rangle+L\frac{\Delta}{\pi\lambda v_F}=0\;. \tag{3.23}$$

Using the relation

$$\int dx\langle\Psi_s^{\dagger}(x)\sigma_1\Psi_s(x)\rangle=2NT\sum_{n}g_2(iE_n)\;, \tag{3.24}$$

and introducing the spectral representation

$$g_2(iE_n)=\int_{-\infty}^{\infty}dx\frac{\tau(x)}{iE_n-x}\;, \tag{3.25}$$

we rewrite (3.23) as

$$\Delta=-4\pi\lambda t_0\int_{-\infty}^{\infty}dx\,f(x)\tau(x)\;, \tag{3.26}$$

where $f(x)=1/[\exp(x/T)+1]$ and

$$\tau(x)=-\frac{1}{\pi}\mathrm{Im}g_2(x+i\delta)\;, \tag{3.27}$$

since $\tau(x)$ is shown to be a real function in Appendix B. At $T=0$, Eq. (3.26) becomes

$$\Delta=-4\pi\lambda t_0\int_{-\infty}^{0}dx\,\tau(x)\;. \tag{3.28}$$

IV. NUMERICAL RESULTS

In the numerical investigations, we use the parameters $t_0=2.5$ eV, $v_F\Lambda=2t_0$, and $\lambda=0.183$. The value of I is varied within $0<I\le t_0$ and the impurity concentration is in the range $c\lesssim 0.1$.

We take 283 points in the mesh of ω space. They consist of 41 points for each sign of ω in $1.5|\Delta|<|\omega|\le E_{\mathrm{cut}}$, and 201 points for $|\omega|\le 1.5|\Delta|$, where $E_{\mathrm{cut}}=1.1[(v_F\Lambda)^2+\Delta_0^2]^{1/2}$ and $\Delta_0=2v_F\Lambda\exp(-1/2\lambda)$. In each energy range, they are distributed with equidistance. The finer mesh is used at $|\omega|\lesssim 1.5|\Delta|$, where new band structures would be expected. The upper limit E_{cut} is a little large so as to be able to treat the change of the band edges.

First, we take an arbitrary value for Δ. The two functions, g_1 and g_2, are first determined by (3.21a) with

$\Sigma_1 = \Sigma_2 = 0$. Equation (3.22) is solved to give new $\Sigma_1(\omega + i\delta)$ and $\Sigma_2(\omega + i\delta)$, which give rise to new g_1 and g_2 with the help of (3.21a). The spectral function $\tau(x)$ is calculated by (3.27), which gives a new Δ by (3.28). This process is iterated until the new Δ coincides with the next new Δ within a relative magnitude of 10^{-4}. During the iterations it is checked that the total number of states does not change more than 0.01%.

For $c \lesssim 0.08$, we get three values for Δ, depending on the starting value of Δ. If I is positive, two of the three are negative and the other one positive. For negative I, two of them are positive. In Fig. 1, we plot the two negative Δ's as functions of c for a positive I, with $I = 1.0$ eV $(I/t_0 = 0.4)$. One is shown by the solid line and the other by the dashed line. At $c \gtrsim 0.08$, these two do not exist. In Fig. 2, we plot the positive Δ which exists for all values of c. As c becomes larger, Δ increases. The corresponding energies per site are calculated with the help of the formula

$$E = 2\int_{-\infty}^{0} dx\, x\rho(x) + \frac{\Delta^2}{2\pi\lambda t_0}\ , \qquad (4.1)$$

where $\rho(x)$ is the density of states (DOS) defined by

$$\rho(x) = -\frac{1}{\pi}\mathrm{Im}\,\mathrm{Tr}[\bar{g}(x+i\delta)] = -\frac{2}{\pi}\mathrm{Im}\,g_1(x+i\delta)\ . \qquad (4.2)$$

They are plotted in Fig. 3. The solid curve is for the positive Δ. The dashed and the dash-dotted curves correspond to the solid and dashed lines in Fig. 1, respectively. We find that the two negative Δ's correspond to a local minimum and a maximum of the energy. This situation is similar to that in the Brazovskii-Kirova (BK) model of *cis*-polyacetylene.[15] The positive Δ corresponds to an energy minimum.

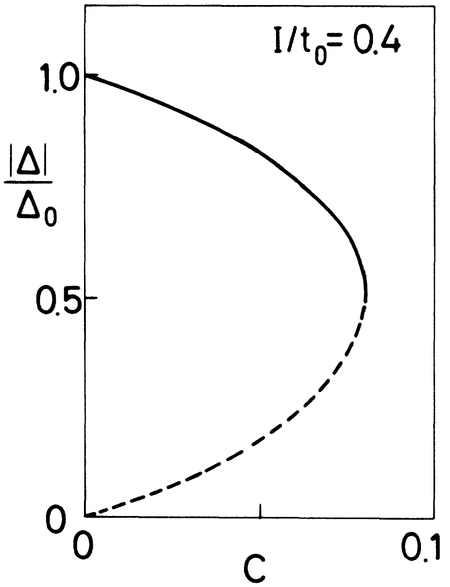

FIG. 1. Negative order parameters. The solid and dashed lines correspond to the metastable and unstable solutions, respectively. The impurity strength is $I = 1$ eV with $I/t_0 = 0.4$. The abscissa is the impurity concentration c.

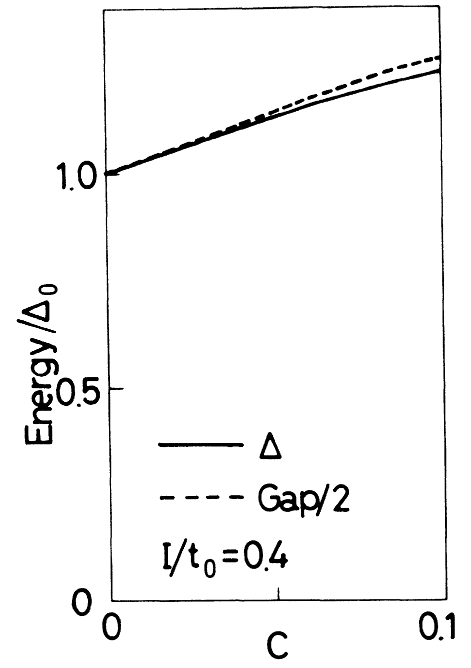

FIG. 2. Positive order parameter and half of the energy gap. They correspond to the stable energy minimum solution. The order parameter is denoted by the solid line. The energy gap is plotted by the dashed line.

The density of states per site (4.2) is shown for the local-minimum solution in Fig. 4. We find that, as c increases, the valence band extends into the gap region due to the generation of an impurity band. Consequently the

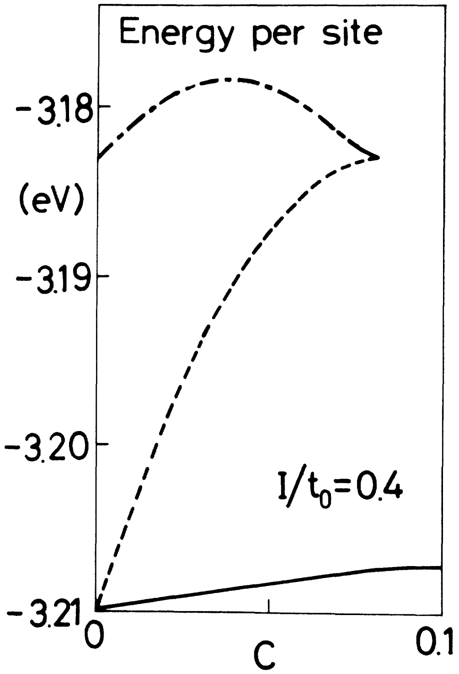

FIG. 3. The energy per site. The dash-dotted line is for the unstable solution. The dashed and solid lines are for the metastable and stable solutions, respectively.

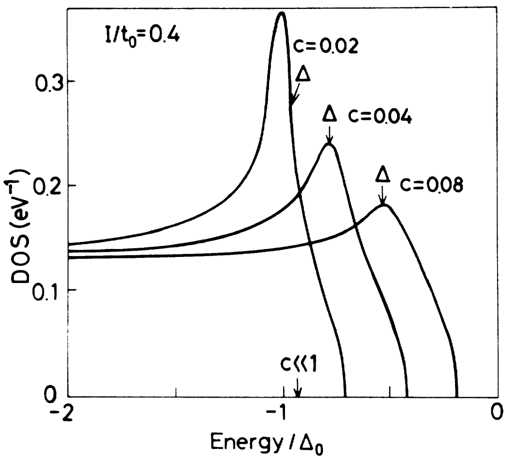

FIG. 4. The density of states per site of the metastable solution. The arrows on the curves indicate the magnitudes of the order parameters. Due to the electron-hole symmetry, the density of states is symmetric with respect to the gap center. Only the valence bands are shown. The arrow on the abscissa indicates the location of the localized level in the single impurity problem.

gap width decreases. The c dependence of the gap is plotted in Fig. 5. In Fig. 6, we show the DOS of the energy-minimum solution. No impurity bands develop. As c becomes larger, the gap width increases and the DOS becomes steeper at $|\omega| \sim |\Delta|$.

In Sec. II, we found that the localized electronic states around an impurity exist only if $U\Delta$ is negative. This is the reason why the impurity bands can develop only in the case where $I\Delta$ is negative. Unfortunately, we cannot gain electronic energy by forming impurity bands. Even if the lattice energy becomes smaller, loss in the electronic energy is larger, because of the upward shift of the DOS of the valence band. On the other hand, in the energy-minimum solution, we can gain electronic energy by the downward shift of the DOS. Impurity effects increase the lattice energy, but the gain in the electronic energy is larger. According to the CPA, the *trans*-polyacetylene with bond-type impurities thus has no impurity bands in the gap region.

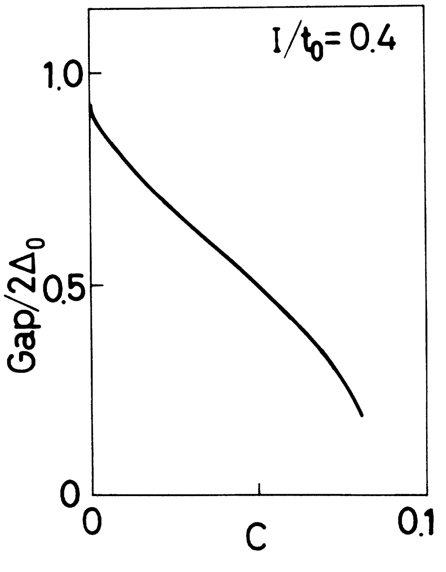

FIG. 5. Half of the energy gap for the metastable solution, as a function of the concentration.

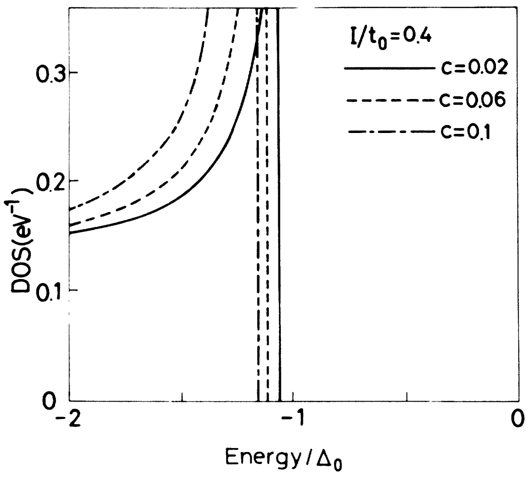

FIG. 6. The density of states per site of the stable solution. Only the valence bands are shown.

We plot the critical concentration c_r, where the local minimum disappears, as a function of impurity strength in Fig. 7. As I increases, it decreases. The figure suggests that c_r is inversely proportional to I. This feature will be discussed further in the next section.

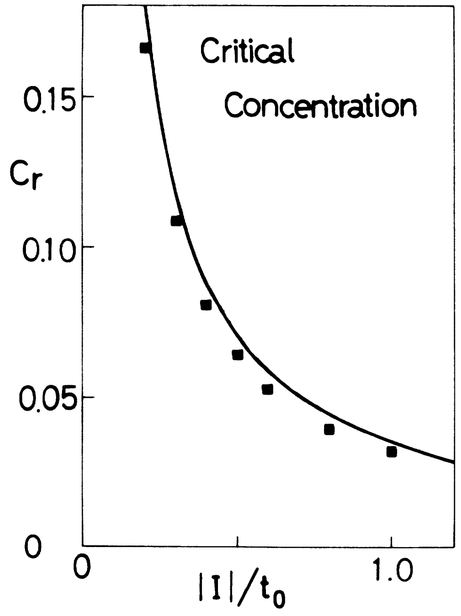

FIG. 7. Impurity strength dependence of the critical concentration c_r for the metastable solution. The squares indicate the numerical results by the CPA. The solid line represents (5.4), which is obtained in the limit of weak impurity strength.

V. DISCUSSIONS

Qualitative features of the numerical results in Sec. IV can be understood in the following way.

In the dilute concentration limit, $c \ll 1$, Eq. (3.22) becomes

$$\Sigma = cI\sigma_1(1-\bar{g}I\sigma_1)^{-1} . \tag{5.1}$$

The strength I is varied within $0 < I \leq t_0$. Equation (3.21a) shows that $\bar{g}$ has the magnitude of the order of t_0^{-1}. Thus, the quantity $\bar{g}I$ is of the order unity. Usually, it is smaller. Thus, in the simplest approximation, we can set $\Sigma = cI\sigma_1$. Then, the difference in the total energies per site, (4.1), between the present state and the undimerized impurity-free state, is calculated to be

$$\delta E = \frac{1}{\pi t_0}(\Delta + cI)^2 \left[\frac{1}{2} + \mathrm{Ln} \left| \frac{\Delta + cI}{2v_F\Lambda} \right| \right] + \frac{\Delta^2}{2\pi\lambda t_0} , \tag{5.2}$$

where the relations $v_F\Lambda \gg \Delta$, cI are used. Here, the term cI plays the role of the extrinsic order parameter Δ_e in the BK model.[15]

Minimizing (5.2), we obtain

$$\frac{\partial \delta E}{\partial \Delta} = \frac{2(\Delta + cI)}{\pi t_0} \mathrm{Ln} \left| \frac{\Delta + cI}{2v_F\Lambda} \right| + \frac{\Delta}{\pi\lambda t_0} + \frac{\Delta + cI}{\pi t_0} = 0 . \tag{5.3}$$

The last term is neglected in the limit of a small λ. The critical concentration, where the local minimum disappears, is obtained with the help of (5.3) and $\partial^2\delta E/\partial\Delta^2 = 0$. We find

$$c_r = \frac{2\lambda}{e} \frac{\Delta_0}{|I|} = 0.135 \frac{\Delta_0}{|I|} , \tag{5.4}$$

and the order parameter has the value

$$|\Delta_c| = \frac{\Delta_0}{e} + c_r|I| = \frac{1+2\lambda}{e}\Delta_0 = 0.503\Delta_0 = 0.327\ \mathrm{eV} \tag{5.5}$$

at the critical concentration.

Equation (5.4) is represented by the solid line in Fig. 7. The agreement with numerical data turns out to be excellent. The small difference between the two results is due to the effect of the impurity bands. Since the contribution from the midgap impurity-band states is neglected in (5.4), the loss in the electronic energy is underestimated. Then, the quantity c_r becomes larger than the numerical result. The value (5.5) agrees very well with that of Fig. 1. Numerical results show that Δ_c does not depend on I strongly.

Earlier works[7–9] on the impurity effects in doped polyacetylene have assumed that the impurity strengths are weak and the concentration is large. Numerical simulations[11] have been performed for doping with compensation. The concentration has been relatively low but the strengths have been strong. Our work corresponds to the latter case with strong impurity strength and small concentration.

These simulations have mainly concentrated on the lattice configurations and vibrations. Information on the electronic band structures has been stored and used in the procedures, but has not been analyzed in detail. It was realized, however, that the bond-type impurities give rise to a density of states which is quite different from the site-type impurities. It is small inside the gap region. A quantitative comparison has to be made in the near future.

One drawback of the present work is the assumption of a uniform dimerization. It has been known that the doping can generate solitons, a process which has been shown also by the numerical simulations. It is difficult to take into account such nonlinear excitations, which break the translational invariance, using the CPA. This method takes an average over the impurity distributions and restores the translational invariance. One possibility to overcome this problem is to study the fluctuation of the dimerization about the uniform value. This effect would lead to quantitative modifications of the present results but is not sufficient to study solitons. It would be necessary to generalize the CPA so as to be able to consider the large variation of the order parameter which takes place locally over a region of the coherence length.

Similarly we can discuss the electronic structure in the presence of site-type impurities[16] or study the simultaneous doping with both types of impurities.[17] These results will be published separately.

Recently, Xu and Taylor informed us that they have analytically solved the problem of a system with a Poisson distribution of impurities and a uniform dimerization, using the supersymmetric techniques.[18] It would give an opportunity to find how effective the CPA is in practice. To know the limit and applicability of the CPA should be quite important when we apply it to the system with a nonuniform dimerization.

ACKNOWLEDGMENTS

One of the authors (Y.W.) would like to thank the University of Bayreuth for their warm hospitality during his visit. Fruitful discussions with Professor Y. Ono, Dr. A. Terai, Dr. K. Iwano, and Mr. K. Yonemitsu are acknowledged. The authors thank Professor P. L. Taylor and Dr. B.-C. Xu for sending them the results prior to publication. This work has been partially supported by a Grant-in-Aid for Scientific Research from the Ministry of Education, Science and Culture, Japan, and by the Research Association for Basic Polymer Technology under the sponsorship of NEDO (New Energy and Industrial Technology Development Organization), Japan. It has also been supported by Deutsche Forschungsgemeinschaft (Bonn, Germany) through SFB (Sonderforschungsbereich) 213 (TOPOMAK, Bayreuth). Numerical calculations have been performed on the Fujitsu FACOM-M-380Q computer of the ICEPP (International Center for Elementary Particle Physics), University of Tokyo.

APPENDIX A: ANALYTICITY OF THE COHERENT POTENTIAL Σ

Analytic properties of Σ are to be examined when the impurity strength I is weak. Expanding (3.22) in a power series of I, we obtain

$$\Sigma = cI\sigma_1 + c(1-c)I\sigma_1 \bar{g} I\sigma_1 + O(I^3) . \tag{A1}$$

The form of $\bar{g}$ in the lowest order is

$$\bar{g}(\omega + i\delta) = g_1 1 + g_2\sigma_1 , \tag{A2}$$

where

$$g_1 = -\frac{i|\omega|}{2t_0(\omega^2-\Delta^2)^{1/2}} , \tag{A2a}$$

and

$$g_2 = -\frac{i\Delta(\mathrm{sgn}\omega)}{2t_0(\omega^2-\Delta^2)^{1/2}} , \tag{A2b}$$

for $|\omega| > |\Delta|$. Substitution of (A2) into (A1) gives

$$\Sigma_1 = -c(1-c)I^2\frac{i|\omega|}{2t_0(\omega^2-\Delta^2)^{1/2}} , \tag{A3a}$$

and

$$\Sigma_2 = cI - c(1-c)I^2\frac{i\Delta(\mathrm{sgn}\omega)}{2t_0(\omega^2-\Delta^2)^{1/2}} . \tag{A3b}$$

These results indicate that Σ has an analyticity appropriate for retarded Green functions, that is, $\mathrm{Im}\Sigma_1 < 0$ and $\mathrm{Im}\Sigma_2/(\omega\Delta) < 0$, in the frequency region $|\omega| > |\Delta|$. The coefficients of I^2 terms of Σ_j's ($j = 1,2$) are $c(1-c)$ which is the second-order cumulant.

APPENDIX B: REALITY OF THE SPECTRAL FUNCTION $\tau(x)$

The definition of the Green function (2.4) leads to the spectral representation

$$G_{sij}(k,p,iE_n) = \frac{1}{Z}\sum_{m,m'}\frac{e^{-\beta\varepsilon_m}+e^{-\beta\varepsilon_{m'}}}{iE_n+\varepsilon_m-\varepsilon_{m'}}\langle m|\Psi_{si}(k)|m'\rangle\langle m'|\Psi_{sj}^{\dagger}(p)|m\rangle , \tag{B1}$$

where Z is the partition function, and ε_m the mth eigenvalue of the one-electron problem (2.1), without the last term of (2.1a), $|m\rangle$ being the corresponding eigenstate, and β is the inverse temperature. If we write

$$[\bar{g}(iE_n)]_{ij} = \int_{-\infty}^{\infty} dx\frac{\tau_{ij}(x)}{iE_n - x} , \tag{B2}$$

the spectral function turns out to be

$$\tau_{ij}(x) = \frac{1}{ZN}\sum_{n,n'}\overline{\delta(\varepsilon_n-\varepsilon_{n'}+x)(e^{-\beta\varepsilon_n}+e^{-\beta\varepsilon_{n'}})\sum_k\langle n|\Psi_{si}(k)|n'\rangle\langle n'|\Psi_{sj}^{\dagger}(k)|n\rangle} , \tag{B3}$$

where the overbar indicates the average over the impurity distribution. It gives

$$\tau_{12} = \tau_{21}^{*} , \tag{B4}$$

which means τ, in (3.25), is real with the help of (3.20).

---

[1] A. J. Heeger, S. Kivelson, J. R. Schrieffer, and W.-P. Su, Rev. Mod. Phys. **60**, 781 (1988).

[2] S. Kivelson, Phys. Rev. B **25**, 3798 (1982); T. Yamabe, K. Tanaka, S. Yamanaka, T. Koike, and K. Fukui, J. Chem. Phys. **82**, 5753 (1985).

[3] H. Fukutome and A. Takahashi, Prog. Theor. Phys. **77**, 1376 (1987).

[4] K. Ehinger and S. Roth, Philos. Mag. B **53**, 301 (1986).

[5] S. R. Phillpot, P. Baeriswyl, A. R. Bishop, and P. S. Lomdahl, Phys. Rev. B **35**, 7533 (1987).

[6] H. Takayama, Y. R. Lin-Liu, and K. Maki, Phys. Rev. B **21**, 2388 (1980).

[7] B.-C. Xu and S. E. Trullinger, Phys. Rev. Lett. **57**, 3113 (1986); *Nonlinearity in Condensed Matter*, edited by A. R. Bishop, D. K. Campbell, P. Kumar, and S. E. Trullinger (Springer, Berlin, 1987), p. 111; B.-C. Xu, J. Phys. Condens. Matter **1**, 3409 (1989).

[8] K. Fesser, J. Phys. C **21**, 5361 (1988).

[9] K. Iwano and Y. Wada, J. Phys. Soc. Jpn. **58**, 602 (1989).

[10] A. Terai, doctoral thesis, University of Tokyo (1988).

[11] Y. Ono, K. Iwano, A. Terai, Y. Ohfuti, and Y. Wada, J. Phys. Soc. Jpn. **58**, 2450 (1989); K. Iwano, Y. Ono, A. Terai, Y. Ohfuti, and Y. Wada, *ibid.* **58**, 4048 (1989).

[12] I. Tüttö and A. Zawadowskii, Phys. Rev. B **32**, 2449 (1985).

[13] H. Shiba, Prog. Theor. Phys. **40**, 435 (1968).

[14] F. Yonezawa and K. Morigaki, Suppl. Prog. Theor. Phys. **53**, 1 (1973); J. M. Ziman, *Models of Disorder* (Cambridge University Press, Cambridge, 1979), Chap. 9.

[15] S. A. Brazovskii and N. N. Kirova, Pis'ma Zh. Eksp. Teor. Fiz. **33**, 6 (1981) [JETP Lett. **33**, 4 (1981)].

[16] K. Harigaya, Y. Wada, and K. Fesser, following paper, Phys. Rev. B **42**, 1276 (1990).

[17] K. Harigaya, Y. Wada, and K. Fesser, Phys. Rev. Lett. **63**, 2401 (1989).

[18] B.-C. Xu and P. L. Taylor (private communication).